REGOLITH DEPTH, MOBILITY, AND VARIABILITY ON VESTA FROM DAWN'S LOW ALTITUDE MAPPING ORBIT. B. W. Denevi[1], E. I. Coman[1], D. T. Blewett[1], D. W. Mittlefehldt[2], D. L. Buczkowski[1], J.-P. Combe[3], M. C. De Sanctis[4], R. Jaumann[5], J-Y. Li[6], S. Marchi[7], A. Nathues[8], N. E. Petro[9], C. M. Pieters[10], P. Schenk[11], N. Schmedemann[12], S. Schröder[8], J. M. Sunshine[6], D. A. Williams[13], C. A. Raymond[14], and C. T. Russell[15]. [1]Johns Hopkins University Applied Physics Laboratory, Laurel, MD, USA, [2]NASA Johnson Space Center, Houston, TX, USA, [3]Bear Fight Institute, Winthrop, WA, USA, [4]INAF, Istituto di Astrofisica e Planetologia Spaziali, Rome, Italy, [5]DLR, Institute of Planetary Research, Berlin, Germany [6]University of Maryland, College Park, MD, USA, [7]NASA Lunar Science Institute, Boulder, CO, USA, [8]Max Planck Institute for Solar System Research, Katlenburg-Lindau, Germany, [9]NASA Goddard Space Flight Center, Greenbelt, MD, USA, [10]Brown University, Providence, RI, USA, [11]Lunar and Planetary Institute, Houston, TX, USA, [12]Freie Universität, Berlin, Germany, [13]Arizona State University, Tempe, AZ, USA, [14]Jet Propulsion Laboratory, California Institute of Technology, Pasadena, CA, USA, [15]University of California, Los Angeles, CA, USA.

Introduction: Regolith, the fragmental debris layer formed from impact events of all sizes, covers the surface of all asteroids imaged by spacecraft to date. Here we use Framing Camera (FC) images [1] acquired by the Dawn spacecraft [2] from its low-altitude mapping orbit (LAMO) of 210 km (pixel scales of ~20 m) to characterize regolith depth, variability, and mobility on Vesta, and to locate areas of especially thin regolith and exposures of competent material. These results will help to evaluate how the surface of this differentiated asteroid has evolved over time, and provide key contextual information for understanding the origin and degree of mixing of the surficial materials for which compositions are estimated [3,4] and the causes of the relative spectral immaturity of the surface [5]. Vestan regolith samples, in the form of howardite meteorites, can be studied in the laboratory to provide complementary constraints on the regolith process [6].

Observations of crater walls: FC images reveal exposures of competent material and layers within crater walls (Fig. 1). Many craters show a spur and gully erosional pattern, with spurs appearing to originate at the surface in some cases (Fig. 1A). This morphology is consistent with mass wasting of materials downslope, and indicates material resistant to erosion near to the surface. If this material represents a layer of competent or fractured rock, this would indicate regolith thicknesses in these regions of < 20-40 m for images acquired at 20 m/pixel. However, regolith near crater rims is likely thinner than typical intercrater regions, as it is more easily sloughed into the crater itself. We also find evidence for layers resistant to erosion several hundred meters below the surface (Fig. 1B). In the case in Fig. 1B, a ledge with a possible overhang of material is also visible at the surface. Many of the craters that expose such materials are found within the Rheasilvia impact basin [7], and we are working to map the global distribution of these occurrences.

Blocky ejecta: One standard technique for estimating regolith depth is to identify the presence (or lack) of blocks in crater ejecta; this technique was first applied to Surveyor I images of the Moon [8]. This method assumes that craters without blocky ejecta formed solely within the unconsolidated regolith, and when blocks are present, they were excavated from the more competent substrate beneath the regolith. At pixel scales of ~18 m, FC images can be used to identify locations where craters have penetrated especially competent material to excavate blocks, but cannot resolve whether blocks are present at small craters and thus cannot help to constrain minimum regolith depths.

Blocky ejecta is observed around many craters on Vesta (Fig. 2). The smallest crater with positive block identification thus far is ~3.3 km in diameter (Fig. 2C), with blocks detected but not clearly resolved (<~30 m), consistent with the largest blocks expected for a crater of this size [9]. We have begun to map the distribution of blocks on the surface of Vesta using LAMO images in an effort to search for variations in regolith among different geologic units [10].

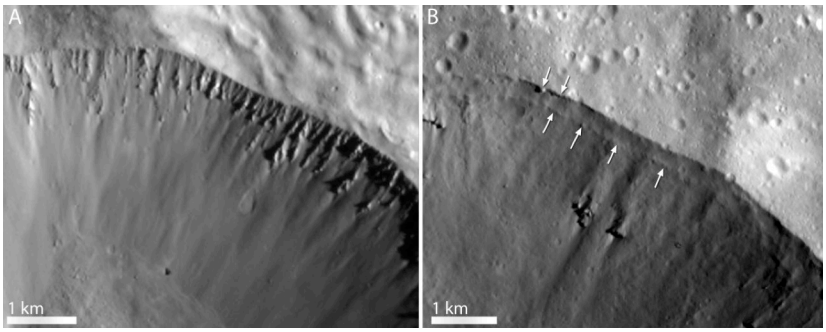

Fig. 1. Examples of exposures of coherent material within crater walls. A) The wall of a ~15 km crater centered at 58.7° S, 200.7° E (image FC21A0014923_11355163605F1). B) A resistant layer ~250 m below surface (lower arrows) and a possible resistant layer and overhang of material at the surface (upper arrows). Crater is ~22 km in diameter, scene centered at 40.0° S, 205.5° E (image FC21A0015710_11361221112F1).

Small Crater Populations: The population of small (< ~200 m) craters has also been shown to be sensitive to regolith depth. For example, the mare has substantially higher densities of small craters as compared to the older highlands, and Eros and Gaspra have been noted to show decreased crater densities below 200 m [11–14]. For areas of thick regolith, the preferential degradation of small craters has been attributed to their formation largely within the thick layer of unconsolidated material [12,14]. The population of small craters in regions of especially thick regolith such as Shoemaker Regio on Eros is similar to the lunar highlands population [14]; we are examining the small crater populations of different geologic [10] and spectral [3,15] units on Vesta for comparison.

Downslope Movement: Numerous examples indicating downslope movement of regolith are found in LAMO images. Regolith is seen to nearly fill craters formed on slopes, indicting local regolith depths of hundreds of meters in these areas. We are examining these occurrences and comparing them to local slopes to examine regolith mobility on Vesta.

Discussion: The lower gravity on Vesta means that material with lower mechanical strength may be resistant to erosion; the question of interest is whether the materials exposed within crater walls are bedrock (likely heavily fractured), or weakly to moderately competent material within the regolith (including ejecta layers or impact melt). If the material is bedrock or fractured rock, it may be exposed by craters in local areas of thin regolith, but the muted topography observed particularly within Rheasilvia suggests most regions are mantled by unconsolidated debris. Global mapping of exposures of this material within crater walls, as well as block populations and comparisons of small crater populations will help elucidate the depth and variations in regolith across geologic units and the surface evolution of these units. Physical properties of the topmost surface derived from near-infrared observations will be also considered [16].

Acknowledgements: This work is supported by NASA's Dawn at Vesta Participating Scientist program, grant number NNX11AC28G.

References: [1] Sierks H. et al. (2011) "The Dawn Framing Camera," *Space Sci. Rev.*, 163, 263-327. [2] Russell C. T. and Raymond C. A., (2011) *Space Sci. Rev.*, 163, 3-23. [3] De Sanctis M. C. et al. (2012) *LPSC 43*, this mtg. [4] Prettyman T. H. et al., (2012) *LPSC 43*, this mtg. [5] Pieters C. M. et al. (2012) *LPSC 43*, this mtg. [6] Mittlefehldt D. W. et al. (2011) *LPSC 42*, abs. 2569. [7] Schenk P. et al. (2011) *AGU Fall Mtg.* U21B-03. [8] Rennilson, J. J. et al. (1966) in *Surveyor I mission report, part II: Scientific data and results, NASA Tech. Report 32-1023*, 7-44. [9] Moore H. J. (1971) in *Analysis of Apollo 10 Photography and Visual Observations, NASA SP-232*, 26. [10] Yingst R. A. et al., (2012) *LPSC 43*, this mtg. [11] Trask N. J. and Rowan L. C. (1967) *Science*, 158, 1529-1535. [12] Carr M. H. et al. (1994) *Icarus*, 107, 67-71. [13] Veverka J. et al. (2001) *Science*, 292, 484-488. [14] Robinson M. S. et al. (2002) *Meteor. Planet. Sci.*, 37, 1651-1684. [15] Nathues A. et al. (2011) *AGU Fall Mtg.* U22A-01. [16] Capria M. T. et al., (2012) *LPSC 43,* this mtg.

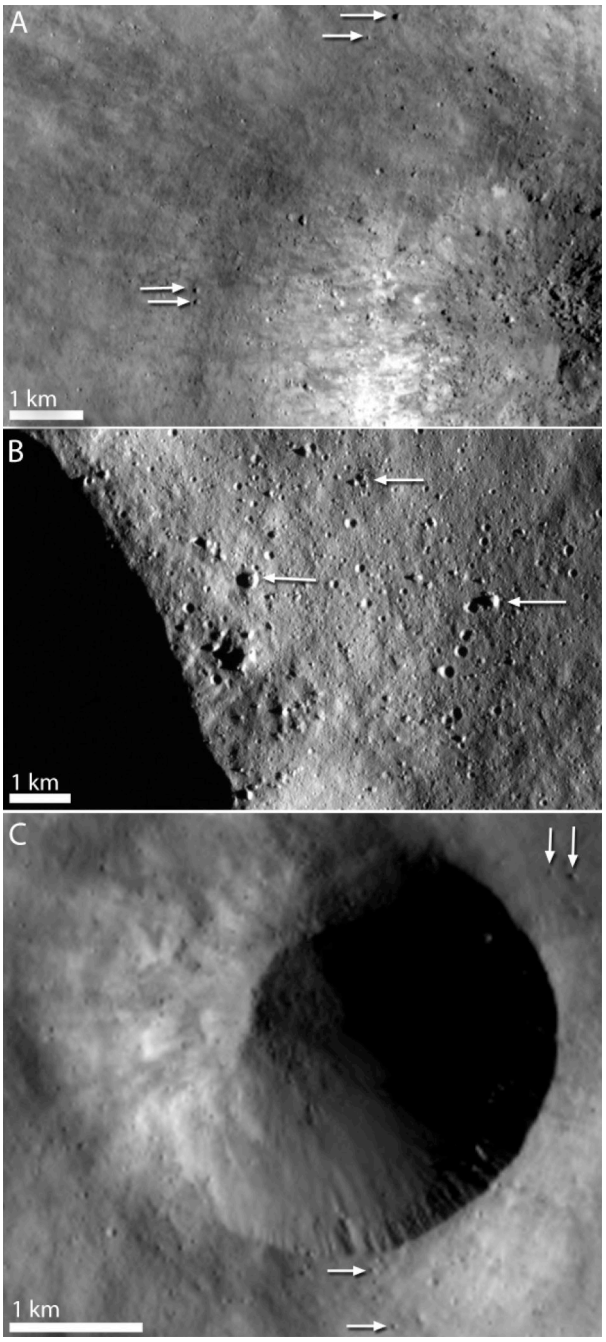

Fig. 2. Examples of blocks in crater ejecta. Arrows highlight selected boulders within the ejecta. A) Blocks surrounding a ~8.8 km diameter crater at 26.9° S, 220.2° E (image FC21A0014744_11354133949F1). B) Blocks up to 250 m in the ejecta of a ~30 km crater, 22.3° N, 20.3° E (image FC21A3014333_11347133750F1). C) Blocky ejecta of a crater ~3.3 km in diameter, 67.5° S, 127.5°E (image FC21A0015660_11361180456F1).